Available online at www.sciencedirect.com
SCIENCE DIRECT®
Journal of Non-Crystalline Solids 348 (2004) 94–97
JOURNAL OF NON-CRYSTALLINE SOLIDS
www.elsevier.com/locate/jnoncrysol

Er^{3+} laser transition in $PbO–PbF_2–B_2O_3$ glasses

L.R.P. Kassab [a,*], L.C. Courrol [a], R. Seragioli [a], N.U. Wetter [b], S.H. Tatumi [a], L. Gomes [b]

[a] *Laboratório de Vidros e Datação, Faculdade de Tecnologia de São Paulo, Centro Est adual de Educacao, Praça Cel. Fernando Prestes 30, CEP 01124-060 São Paulo, SP, Brazil*
[b] *Centro de Lasers e Aplicações, IPEN-CNEN, São Paulo, SP, Brasil*

Abstract

Results of absorption, emission and fluorescence lifetime measurements (for the $^4I_{13/2} \rightarrow {}^4I_{15/2}$ transition) are presented for lead fluoroborate glasses doped with different concentrations of Er^{3+} varying from 0.22×10^{20} ions/cm^3 to 5.96×10^{20} ions/cm^3. The calculated Judd–Ofelt parameters are: $\Omega_2 = (1.2 \pm 0.1) \times 10^{-20}$ cm^2, $\Omega_4 = (0.59 \pm 0.04) \times 10^{-20}$ and $\Omega_6 = (0.42 \pm 0.03)\ 10^{-20}$ cm^2. The emission cross-sections are calculated using McCumber and Fuchtbauer–Ladenburg methods. The sample with 2.20×10^{20} ions/cm^3 has an emission cross-section with maximum of 0.46×10^{-20} cm^2, at 1532 nm, fluorescence effective bandwidth of 66 nm and fluorescence lifetime of about 1 ms.

PACS: 42.70.–a

1. Introduction

When erbium ions are presented in a glass material, they have emission bands located at about 1500 nm and 2700 nm [1]. The first one coincides with the third telecommunication window [2]; this transition provides amplification near 1540 nm in erbium doped fiber amplifiers and radiation for eye safe remote sensing applications [3]. The second emission band has interest for optical sources for sensors and for medicine [4].

$PbO–PbF_2–B_2O_3$ glasses are of interest in optoelectronic devices due to their properties: transmission window from 400 nm to 4 μm, high refractive index of about 2.2 and good physical and chemical stability. We reported the results of this host doped with Yb^{3+} [5–7], Nd^{3+} [8], and codoped with Yb^{3+} and Er^{3+} [9]. Now, we present studies of the $^4I_{13/2} \rightarrow {}^4I_{15/2}$ laser transition in lead fluoroborate glasses $PbO–PbF_2–B_2O_3$, doped with different concentrations of Er_2O_3. Results of absorption, fluorescence lifetime and emission are presented as well as Judd–Ofelt calculations. Comparisons with other known laser glasses are also made.

2. Experiment

The samples were produced at the Laboratory of Glasses and Datation at the Faculty of Technology of São Paulo using the following glass matrix: $38.8B_2O_3$–$27.1PbO$–$34.1PbF_2$ mol%). After melting the powders in Pt crucibles at 1000 °C for 1 hour and a half, they are poured into heated brass molds (300 °C), annealed for 3 h at 300 °C (transition temperature is 380 °C) and then cooled inside the furnace after the furnace is turned off. The refractive index of (2.20 ± 0.05) was determined by means of the 'apparent depth method' that relates the physical thickness of the samples to their optical thickness (apparent thickness). The optical thickness is

* Corresponding author.
E-mail address: kassablm@osite.com.br (L.R.P. Kassab).

0022-3093/$ - see front matter © 2004 Elsevier B.V. All rights reserved.
doi:10.1016/j.jnoncrysol.2004.08.132

measured with a 10× objective lens of a microscope (Carl Zeiss). The absorption spectra at room temperature was recorded with a spectrometer (Cary 500) in the 920–1120 nm range. The density of (7.0 ± 0.1) g/cm^3 was measured with the Archimedes method. The emission spectra was measured using an excitation beam of 968 nm from a AlGaAs laser diode (Optopower A020). The emission was analyzed with a 0.5 m monochromator (Spex), detected by a Ge detector and intensified with a lock-in amplifier (EG & G7220). The fluorescence was collected 90° from the beam ensuring a shorter path through the glass to reduce reabsorption. The lifetime of the excited Er^{3+} ions was measured using a pulsed laser excitation (4 ns) at 800 nm from an Optical Parametric oscillator (OPO from Opotek) pumped by a frequency doubled Nd:YAG laser (Quantel) with an InSb detector with specific line filters using a signal processing box-car averager (PAR 4402). Errors in these emission and fluorescence lifetime measurements are ±5%.

3. Results

For the absorption measurements we obtained the spectrum shown in Fig. 1 (the thickness of the sample is 4.3 mm). In this spectrum we observe nine bands related to the absorption of Er^{3+} from the $^2G_{9/2}$, $^4F_{3/2}$ + $^4F_{5/2}$, $^4F_{7/2}$, $^2H_{11/2}$, $^4S_{3/2}$, $^4F_{9/2}$, $^4I_{9/2}$, $^4I_{11/2}$ and $^4I_{13/2}$ transitions. The fluorescence lifetimes, measured for the $^4I_{13/2} \rightarrow {}^4I_{15/2}$ transition, were fitted to a single exponential function and the results are shown in Table 1.

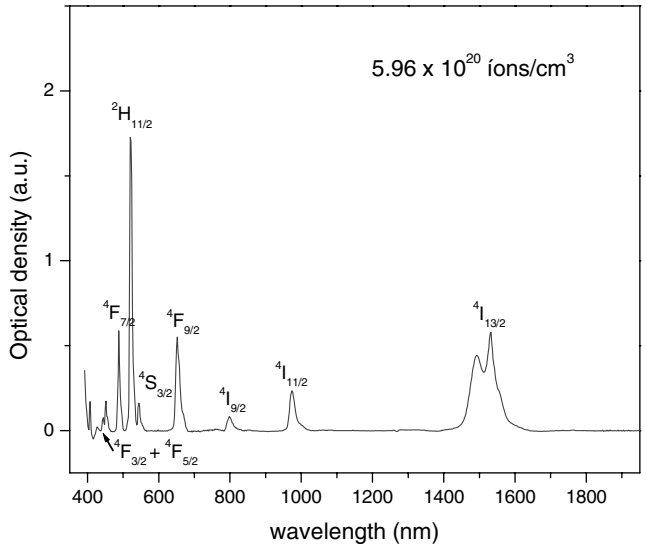

Fig. 1. Absorption spectrum (sample thickness of 4.3 mm) at room temperature for the lead fluoroborate glass ($PbO–PbF_2–B_2O_3$) doped with Er^{3+}.

Table 1
Spectroscopic properties for the fluoroborate glass ($PbO–PbF_2– B_2O_3$) doped with different concentrations of Er^{3+}

Concentration of Er $^{3+}$ (10^{20} ions/cm^3)	Fluorescence lifetime (ms) ($^4I_{13/2} \rightarrow {}^4I_{15/2}$)	σ_{em} ($\times 10^{-20}$ cm^2) ($^4I_{13/2} \rightarrow {}^4I_{15/2}$)	Fluorescence effective linewidth (nm)
0.22	0.99 ± 0.05	0.50 ± 0.08	60.0
1.10	0.99 ± 0.05	0.50 ± 0.08	61.0
2.20	0.99 ± 0.05	0.46 ± 0.07	66.0
5.96	0.67 ± 0.03	0.42 ± 0.07	73.0

Maximum emission cross-section is at 1532 nm, calculated with F–L method.

The Judd–Ofelt parameters (Ω_t) were calculated with the expression below [with the absorption bands, shown in Fig. 1, of the electronic transitions of Er^{3+} from the initial manifold (S, L, J) to the final manifold (S', L', J') that equates the experimental to the calculated oscillator strength for induced electric and magnetic dipole transitions [10]:

$$\frac{mc^2}{\pi e^2 \rho \lambda_p^2} \int k(\lambda) d\lambda = \frac{8\pi^2 mc}{3h(2J+1)\lambda_p} \left(\frac{(n^2+2)^2 S_{ed}}{9n} + n S_{md} \right), \quad (1)$$

where c represents the velocity of light (in cm/s), n the refractive index, ρ the concentration of Er^{3+} ions (in ions/cm^3), λ_p the absorption peak wavelength (in cm), e and m respectively the electron charge and the mass, $k(\lambda)$ the absorption coefficient (in cm^{-1}), S_{ed} and S_{md} represent the line strengths (in cm^2) for the induced electric and magnetic dipole transition, respectively. The line strength for the induced electric dipole (S_{ed}) transition is given by [10]:

$$S_{ed} = \sum_{t=2,4,6} \Omega_t \, | \langle SLJ \| U^t \| S'L'J' \rangle |^2, \quad (2)$$

where $|\langle SLJ \| U^t \| S'L'J' \rangle\|^2$ is the square of the matrix elements of the tensional operator, U^t which connects SLJ to $S'L'J'$ states (determined from the literature [11]).

Because the magnetic dipole oscillator strength of the $^4I_{15/2} \rightarrow {}^4I_{13/2}$ transition has an effect on the total radiative transition it has to be considered in the calculation of the Judd–Ofelt parameters. In Eq. (1) the oscillator strength for the magnetic dipole transition is given by:

$$f_{md} = \frac{8\pi^2 mc S_{md} n}{3h(2J+1)\lambda_p} = f' n, \quad (3)$$

where $f' = 30.82 \times 10^{-8}$ [12] for the $^4I_{15/2} \rightarrow {}^4I_{13/2}$ transition of Er^{3+}. Considering $n = 2.20 \pm 0.05$, f_{md} is $(67 \pm 2) \times 10^{-8}$. The three Judd–Ofelt parameters are determined by a least square fitting routine that compares the measured oscillator strengths for the different Er^{3+} absorption bands with the theoretical oscillator

strengths using the matrix elements tabulated in [11]. The parameters are: $\Omega_2 = (1.2 \pm 0.1) \times 10^{-20}\,\mathrm{cm}^2$, $\Omega_4 = (0.59 \pm 0.04) \times 10^{-20}\,\mathrm{cm}^2$ and $\Omega_6 = (0.42 \pm 0.03) \times 10^{-20}\,\mathrm{cm}^2$. These parameters do not vary with Er^{3+} concentration.

The spontaneous emission probability, from the initial manifold $(S,L,J = 13/2)$ to the final manifold $(S',L',J' = 15/2)$ was determined with the following equation [10]:

$$A_R = \frac{64\pi^4 e^2}{3h(2J+1)\lambda^3}\left(\frac{n(n^2+2)^2 S_{ed}}{9} + n^3 S_{md}\right). \quad (4)$$

In the equation above, λ is the emission peak wavelength.

The peak emission cross-section for the Er^{3+}, $^4I_{13/2} \rightarrow {}^4I_{15/2}$ transition, is expressed using the Fuchtbauer–Ladenburg (F–L) formula [13]:

$$\sigma_{em} = \frac{\lambda^4 A_R}{8\pi n^2 c \Delta\lambda_{EFF}}, \quad (5)$$

where $\Delta\lambda_{EFF}$ is the effective fluorescence bandwidth. Fig. 2 shows the emission cross-section as a function of λ for the sample doped with 2.20×10^{20} ions/cm^3 of Er^{3+}. To confirm the results obtained from Judd–Ofelt theory and F–L formula, for all the cases, the emission cross-sections were calculated using Mc Cumber theory [14]:

$$\sigma_{emi}(\lambda) = \sigma_{abs}(\lambda)\frac{Z_l}{Z_u}\exp\left(\frac{E_{zl} - hc\lambda^{-1}}{kT}\right), \quad (6)$$

where k and E_{zl} are the Boltzman's constant and the zero line energy that is defined as the energy separation between the lowest components of the upper and lower states, respectively. E_{zl} is associated with the most intense peak in the absorption spectrum of Er^{3+} doped glass. A good agreement is observed for the two methods (Fig. 2); the differences are attributed to the reabsorption caused by the spectral overlap of the emission and absorption bands of Er^{3+}, at 1532 nm.

Table 1 summarizes the results obtained for all the samples produced and Table 2 compares the sample doped with 2.20×10^{20} ions/cm^3 of Er^{3+} with the results of recently published papers [15–18].

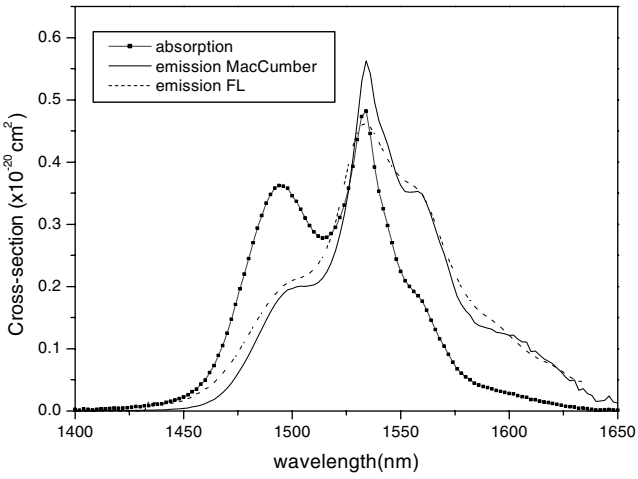

Fig. 2. Absorption and emission cross-sections spectra for the lead fluoroborate glass ($PbO–PbF_2–B_2O_3$) doped with 2.20×10^{20} ions/cm^3 of Er^{3+}. Emission cross-sections are calculated using McCumber theory (solid line) and F–L formula with the Judd–Ofelt parameters (dashed line); the maximum emission cross-section is at 1532 nm.

4. Discussion

As Jorgensen et al. reported that [19], the Ω_2 parameter is affected by covalent chemical bonding and the Ω_4 and Ω_6 parameters are associated to the rigidity of the medium in which the ions are situated. The Ω_2 may be affected by the micro-structural homogeneity around the Er^{3+} ions; a large number of different sites in glasses and lower symmetry in which the rare-earth ion is situated contribute to a high Ω_2 [20]. So the fact that $\Omega_2 < 2.0$ indicates small covalence in bonding and a high degree of homogeneity [20,21]. According to Eq. (2), Ω_6 affects the cross-section of the 1500 nm band more than the other two parameters. As S_{ed} contributes to a broader component of the 1500 nm band, larger Ω_6 and refractive index produce larger emission-cross-sections. However, in our case, whereas the refractive index is (2.20 ± 0.05), Ω_6 is smaller than 0.5×10^{-20} cm^2. That is why the emission cross-section is comparable to ZBLAN and silicate glasses (Table 2) that have considerable smaller refractive indices (1.58 for the first and 1.46 for the second one) but $\Omega_6 > 1$. For example, $\Omega_6 = 1.17 \times 10^{-20}\,\mathrm{cm}^2$ for ZBLAN. Concerning the

Table 2
Spectroscopic properties of some laser glasses and the one studied in this work

Glass composition	Concentration (10^{20} ions/cm^3)	σ_{em} ($\times 10^{-20}$ cm^2) ($^4I_{13/2} \rightarrow {}^4I_{15/2}$)	Fluorescence lifetime (ms) ($^4I_{13/2} \rightarrow {}^4I_{15/2}$)	Refractive index
Ge–Ga–S [15]	0.2	1.05	2.9	2.15
ZBLAN [16]	5.0	0.58	9.0	1.50
4PB [17]	3.0	0.90	1.7	2.27
Silicate [18]	0.7	0.44	10.2	1.46
$PbO–PbF_2–B_2O_3$	2.2	0.46 ± 0.07	0.99 ± 0.05	2.20 ± 0.05

Maximum emission cross-section and fluorescence lifetime are for the ($^4I_{13/2} \rightarrow {}^4I_{15/2}$) transition (at about 1530 nm).

4PB glass (a halotellurite glass) [17], although its refractive index (2.27) is comparable to that of $PbO–PbF_2$-B_2O_3, its emission cross-section is larger (0.90×10^{-20} cm^2) because its Ω_6 is larger ($\Omega_6 = 1.67 \times 10^{-20} cm^2$).

Table 1 shows that the fluorescence lifetimes remain constant up to 2.20×10^{20} ions/cm^3 of Er^{3+} and then, with increasing Er^{3+} concentration, they decrease. We should add that the lifetime decreases to (0.67 ± 0.03) ms, at 5.96×10^{20} ions/cm^3. This shorter fluorescence lifetime can be attributed to non-radiative processes [17,20]: energy migration among Er^{3+} ions, followed by transfer to recombination centres, interaction between Er^{3+} ions and the glassy host defects, trapping by defects such as OH^-. The calculated emission cross-sections present variations of the experimental errors order.

To provide larger laser gain an efficient host for Er^{3+} laser operation should have, as large as possible, the emission cross-section and the capacity to incorporate concentrations of the trivalent rare-earth; longer fluorescence lifetime to minimize pump losses incurred from spontaneous emission is also necessary.Based on these considerations and considering the experimental errors we note that the sample with 2.20×10^{20} ions/cm^3 has adequate spectroscopic properties for laser applications.

Table 2 [15–18] compares the sample doped with 2.20×10^{20} ions/cm^3 of Er^{3+} with the results of recently published papers. We observe that the emission cross-section of the glass samples presented in this work is similar to the ones of ZBLAN [16] and silicate glasses [18]; the fluorescence lifetime is the smallest one. We remark that the refractive index is one of the largest in this group of glasses and indicates a fast non-linear optical behavior [22].

5. Conclusions

$PbO–PbF_2–B_2O_3$ glasses doped with Er^{3+} have a small covalence in bonding and a small number of different sites indicated by the value of Ω_2 ($\Omega_2 < 2.0$). The high refractive index indicates a fast non-linear optical behavior and the possibility for photonic applications.The emission cross-sections were calculated using F–L formula and McCumber theory and a good agreement was verified. The glass doped with 2.20×10^{20} ions/cm^3 of Er^{3+} has suitable spectroscopic properties for laser action related to the $^4I_{13/2} \rightarrow {}^4I_{15/2}$ transition (1532 nm): emission cross-section of $0.46 \times 10^{-20} cm^2$, comparable to ZBLAN and silicate glasses, fluorescence lifetime of 1.0 ms and fluorescence effective linewidth of 66 nm.

Acknowledgment

We thank FAPESP and Laboratório de Datação e Cristais Iônicos/IFUSP

References

[1] Z.X. Cheng, S.J. Zhang, F. Song, H.C. Guo, J.R. Han, H.C. Chen, J. Phys. Chem. Solids 63 (2002) 2011.
[2] R. Rolli, M. Montagna, S. Chaussedent, A. Monteil, V.K. Tikhomirov, M. Ferrari, Opt. Mater. 21 (2003) 743.
[3] A.F. Obaton, C. Parent, G. Le Flem, P. Thony, P. Thony, A. Brenier, G. Boulon, J. Alloy Compd. 300 (2000) 123.
[4] M. Pollnau, S.D. Jackson, IEEE J. Sel. Top. Quantum Electron. 7 (2001) 30.
[5] L.R.P. Kassab, L.C. Courrol, A.S. Morais, et al., J. Non-Cryst. Solids 304 (2002) 233.
[6] L.R.P. Kassab, L.C. Courrol, N.U. Wetter, et al., J. Alloy Compd. 344 (2002) 264.
[7] L.R.P. Kassab, S.H. Tatumi, A.S. Morais, et al., Opt. Express 8 (2001) 585.
[8] L.R.P. Kassab, L.C. Courrol, V.D. Cacho, et al., J. Lumin. 102&103 (2003) 101.
[9] L.R.P. Kassab, L.C. Courrol, A.S. Morais, et al., J. Opt. Soc. Am. B 19 (2002) 2921.
[10] N. Spector, Chem. Phys. Lett. 49 (1977) 49.
[11] M.J. Weber, Phys. Rev. 157 (1967) 157.
[12] W.T. Carnall, P.R. Fields, K. Rajnak, J. Chem. Phys. 49 (1968) 4412.
[13] P.F. Moulton, J. Opt. Soc. Am. B 3 (1986) 125.
[14] D.E. McCumber, Phys. Rev. 136 (1964) A954.
[15] D. Coleman, S.D. Jackson, et al., J. Opt. Soc. Am. B 19 (2002) 1982.
[16] L. Zhang, H. Hu, F. Lin, Mater. Lett. 45 (2001) 189.
[17] Y. Ding, S. Jiang, et al., Opt. Mater. 15 (2002) 123.
[18] W.L. Barnes, R.I. Laming, et al., IEEE J. Quantum Eletron. 27 (1991) 1004.
[19] C.K. Jorgensen, R. Reisfeld, J. Less-Common Met. 93 (1983) 107.
[20] Q. Chen, M. Ferraris, Y. Menke, D. Milanese, E. Monchiero, J. Non-Cryst. Solids 324 (2003) 1.
[21] A. Florez, Y. Messaddeq, O.L. Malta, M.A. Aegerter, J. Alloy Compd. 227 (1995) 135.
[22] S. Smolorz, I. Kang, F. Wise, B.G. Aitken, N.F. Borrelli, J. Non-Cryst. Solids 256 (1999) 310.